PORTABLE, NEAR-INFRARED SPECTROPHOTOMETER
FOR RAPID SOIL ANALYSIS

K. A. Sudduth,   J. W. Hummel

MEMBER   MEMBER
ASAE   ASAE

ABSTRACT. *A portable, near-infrared spectrophotometer was designed, fabricated, and performance tested. Significant features included a circular variable filter monochromator, a fiber optic coupling for sensing of remote samples, and a software algorithm which corrected the instrument readings to a zero baseline. The instrument had a sensing range of 1650 nm to 2650 nm, an optical bandwidth of under 55 nm, and could acquire a spectrum every 200 ms. The intended use of this device was for rapid estimation of soil organic matter as a control input for variable rate herbicide application.*
Keywords. *Soil organic matter, Herbicides, Spectrophotometry, Variable rate application, Optics, Sensors.*

Site-specific crop production, or "prescription farming", is a management technique in which the application rates of such inputs as herbicides and fertilizers are varied within a field in response to spatial differences in soil and agronomic properties. Data quantifying these spatial differences could be collected by intensive sampling and subsequent laboratory analysis, but for highest efficiency it would be desirable to obtain these data by means of automated instruments capable of conducting analyses in the field.

Spectral reflectance measurements provide one possible means for estimating soil properties in the field. Researchers have correlated soil properties with both visible and near infrared (NIR) reflectance data (Dalal and Henry, 1986; Gaultney et al., 1989; Gunsaulis et al., 1991; Henderson et al., 1989; Krishnan et al., 1980; and Schreier, 1977). Sudduth and Hummel (1991) evaluated visible and NIR reflectance data for estimation of the organic matter content of Illinois soils. NIR data analyzed by partial least squares regression provided the best correlations ($r^2 = 0.92$, standard error of prediction 0.34% organic matter) for 30 soils at wilting point and field capacity moisture levels. The reflectance data used were from 1720-2380 nm on a 60-nm spacing and bandwidth, for a total of 12 reflectance points.

This article describes the design, development, and evaluation of a rugged, portable NIR spectrophotometer

that implemented the soil organic matter estimation method chosen by Sudduth and Hummel (1991). The intended use of this instrument was to provide control input data for varying the rates of soil applied herbicides within a field in response to organic matter variations. The NIR spectrophotometer might also be used to quantify spatial variations in other properties, such as soil moisture, that are important in site-specific crop production.

OBJECTIVES

The overall design objective for the prototype spectrophotometer was to implement the optimum soil organic matter prediction method chosen by Sudduth and Hummel (1991) on a near, real-time basis. Specific design sub-objectives were to:

- Utilize a bandpass of 60 nm or less over a minimum sensing range from 1700 nm to 2420 nm.
- Provide an essentially continuous (in wavelength) sensing method, to allow flexibility for additional optimization of the wavelengths selected.
- Have potential, with additional refinements if needed, to generate an organic matter signal every 4.5 s to support on-the-go herbicide application rate adjustment at realistic field speeds.
- Predict soil organic matter content with a standard error of prediction of less than 0.5% (or less than 0.29% organic carbon) for the 30 Illinois soils in the calibration dataset (Sudduth and Hummel, 1991).
- Tolerate harsh environmental conditions (e.g., dust, temperature fluctuations, shock loads, and vibration) that would be encountered in field operation.

SELECTION OF DESIGN ALTERNATIVES

Commercial NIR instruments were surveyed in an attempt to identify a unit meeting the design objectives. The available grating monochromator and tilting filter instruments measured reflectance at more wavelengths than required and at a narrower bandwidth, and this excess capability resulted in high costs. Additionally, these instruments were not designed for the environmental stresses imposed by field operation, and would have been

limited to laboratory use. Available fixed-filter instruments were more rugged and less expensive, but obtained reflectance measurements at a slower rate and at fewer wavelengths than required. Since no commercially available NIR instrument met all the design objectives, development of a prototype spectrophotometer specifically targeted at NIR reflectance sensing of soil organic matter content was necessary.

The wavelength selection mechanism and photodetector were chosen first, since these components would dictate the configuration of the remainder of the system. The alternatives for the photodetector were a single element detector or an array detector. A single element detector would be used with a wavelength selection mechanism (in this case, a monochromator) which scanned the wavelengths of interest sequentially onto the detector. An array detector would be used if the wavelength selection mechanism (in this case, properly termed a spectrograph but usually called a monochromator) focused the wavelengths of interest into a line image on a flat focal plane, thus providing simultaneous sensing at all wavelengths.

Three design alternatives were considered for the wavelength selection mechanism: a grating mono-chromator, a prism, and a circular variable filter (CVF). The grating monochromator was the usual device used in NIR laboratory spectrophotometers (McClure, 1987), but environmental considerations made its use more difficult in a field instrument. Worner (1989) constructed a visible spectrophotometer using a prism and a linear array detector in an attempt to overcome the environmental problems seen with gratings. Circular variable interference filters, which have spectral characteristics that can be varied by means of physical rotation, have been used in rugged field instruments for portable color measurement (Jauch, 1979) and for airborne infrared spectral measurements (Hovis et al., 1967).

Using the above detector and monochromator alternatives, five possible options were identified: 1) Grating and single detector; 2) grating and array detector; 3) prism and single detector; 4) prism and array detector; and 5) CVF and single detector.

Several of these choices were eliminated early in the design process. Option 1, a grating monochromator with a single detector, would require oscillation of the grating to scan all wavelengths of interest onto the detector, making the device prone to vibration-induced inaccuracies. Options 3 and 4 used a prism monochromator, which was not available as a stock item in the wavelength range required. The costs and lead time associated with custom prism design and fabrication were not desirable within the scope of this project. Use of the prism with a single detector would require a scanning mechanism and would entail the same type of vibration problems seen in the grating system. The nonlinear dispersion characteristics of a prism would make it difficult to provide data at equal wavelength spacings with an array detector.

Final consideration then was between Option 2, grating monochromator and array detector, and Option 5, circular variable filter monochromator and single element detector. The circular variable filter monochromator and single element detector combination was selected after a detailed vendor survey, primarily due to the greater flexibility offered by this approach. A CVF was available with a wavelength range of 1600 nm to 2900 nm and a bandwidth of approximately 55 nm (Optical Coating Laboratory, Inc., Santa Rosa, CA). This provided extra capability on both ends of the required sensing range (1700 nm to 2420 nm) while meeting the 60 nm bandwidth requirement. Additional flexibility was realized with the CVF since reflectance readings could be taken at any desired points in the wavelength range, subject only to the limitations of the data acquisition system. In contrast, the best combination of grating monochromator and linear array detector did not completely cover the required range and allowed sensing only from 1720 nm to 2380 nm. This combination had a theoretical bandwidth of 36 nm, but could output only 16 reflectance readings, corresponding to the 16 elements of the linear array detector. Other factors favoring the choice of the CVF system were its greater tolerance of dust and vibration, and a reduced degree of complexity in the interface electronics due to the use of one detector and data channel versus 16 detector elements and channels. One possible drawback of the CVF system was its sequential rather than simultaneous acquisition of data. It was theorized that maximum accuracies with this sequential wavelength scanning approach might require holding the sample stationary while data were being acquired so that all wavelengths were scanned on an identical area of the sample.

DETAILED DESIGN DESCRIPTION

The basic components of the NIR spectrophotometer (fig. 1) were a broadband NIR source, CVF mono-chromator, fiber optic bundle before the sample, and a lead sulfide (PbS) photodetector to measure the energy reflected from the sample. Output of the detector was conditioned by a pre-amplifier and input to a personal computer through an analog-to-digital (A/D) converter.

An aluminum housing formed the main structure of the instrument and enclosed an aluminum filter disk containing the quarter-segment CVF (fig. 2). Modulation of the lamp output radiation for low frequency noise and drift rejection was accomplished with the filter disk itself, rather than by the standard practice of a separate chopper disk. By spinning the filter disk at a sufficient rate and using the three-quarters of the disk which blocked the light path to perform the modulation function, the need for a separate motor, chopping disk, and sensing electronics was avoided. A servo-controlled dc motor-generator (Motomatic E-350, Robbins and Meyers, Hopkins, MN) allowed adjustment of the filter disk rotation speed. Operating speed in this application was limited to 10 Hz due to balancing considerations in the filter disk assembly, photodetector response, and A/D sampling rate.

An opto-interrupter was mounted within the instrument housing such that its optical path was broken once per filter disk revolution by a small tab attached to the circumference of the disk (fig. 2). The timing pulse generated by the opto-interrupter was conditioned to TTL levels by a Schmitt trigger circuit. This TTL signal was then used to compensate for any variations in the filter disk speed and to provide a positive angular position reference for wavelength determination. The timing tab position used initially was opposite the CVF segment. Later tests were
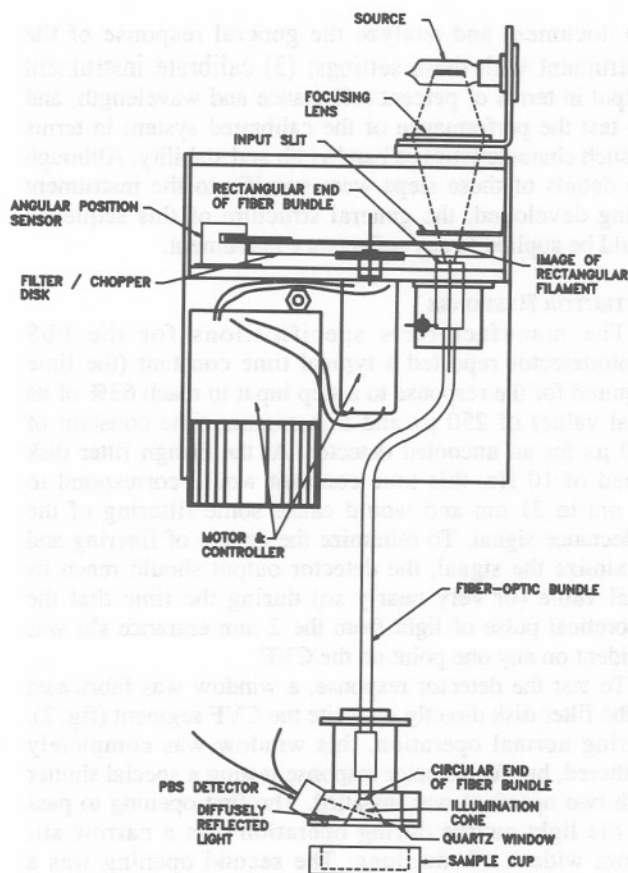
Figure 1–Optical system, including instrument housing with filter disk and lamp (top), and sensor head assembly (bottom).

Figure 2–Circular variable filter disk, including initial and revised timing tab locations.

done with the tab adjacent to the CVF segment on the filter disk (fig. 2) so that the timing pulse would coincide more closely with the analog reflectance signal.

A 50 W, 12 V, quartz halogen automotive-type lamp (fig. 1) driven by a laboratory power supply was used as the illumination source for the spectrophotometer. The lamp mounting allowed three-axis adjustment for focusing and positioning the lamp image. A spherical bi-convex lens (fig. 1) was mounted in the upper surface of the instrument housing to focus the lamp image through the input slit and onto the surface of the CVF.

The wavelength of the light which passed through the CVF at any point in its rotation was a linear function of the angular position of that point relative to the leading edge of the filter. Therefore, to obtain monochromatic (or nearly so) light from the system, a narrow radial slit (2-mm wide × 10-mm radial length) was mounted about 5 mm above the surface of the filter. The projected image of the lamp filament was of a similar size and shape, so that only a small portion of the lamp energy was blocked at the slit.

The monochromatic light from the CVF was directed to the sample through a 610-mm long silica fiber optic bundle with a useful transmission range from 350 nm to over 2400 nm (Volpi Fiber Optics, Auburn, NY). This section converter bundle changed shape from a 1 mm × 10 mm rectangular section at one end to a 3.6 mm circular cross-section at the other. The rectangular section end of the fiber bundle was mounted approximately 5 mm below the surface of the CVF and in line with the input slit, thus

collecting the majority of the filter throughput. The circular cross-section end of the fiber optic bundle was attached to the sensor head assembly with an adjustable mounting, to allow optimization of the location of the fiber exit cone with respect to the detector and the sample surface.

The sensor head assembly (fig. 1) consisted of an aluminum housing, an optically-flat quartz aperture window for dust exclusion, and an attached photodetector. The PbS photodetector was selected as preferable to the other available types (notably lead selenide and indium arsenide) due to its lower cost, higher responsivity, and ability to operate without cooling. Monochromatic light from the fiber optic bundle passed through the quartz aperture window and illuminated a circular area on the sample surface. A portion of the energy diffusely reflected from the sample passed back through the quartz aperture and was collected by the photodetector (OTC-22-53, OptoElectronics, Petaluma, CA). This detector had a useful sensing range from approximately 1000 nm to 3500 nm and a 3 mm × 3 mm square sensing area. The detector was operated uncooled at ambient temperature to ensure an acceptable speed of response. The excitation and preamplifier circuitry (fig. 3) for the PbS detector consisted of a high-gain single stage amplifier which was ac coupled to the output of the detector for insensitivity to low frequency drift in the detector output.
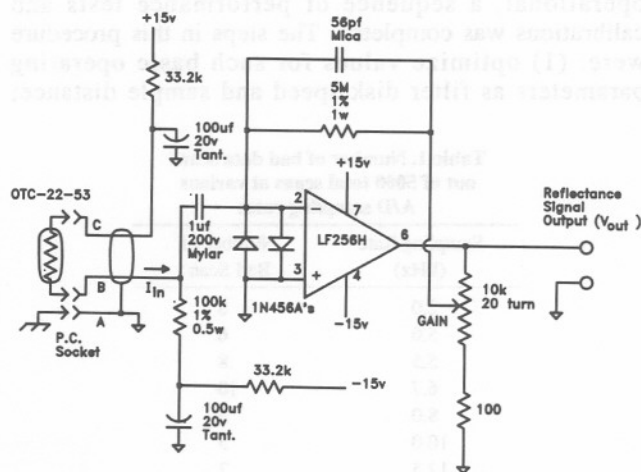
Figure 3–Detector excitation and preamplifier circuit.

DATA ACQUISITION SYSTEM

Data was acquired with a MetraByte DAS-16 analog and digital input-output expansion board (Keithley, Taunton, MA) installed in an AT-compatible computer running at 12 MHz. One 12-bit differential analog channel on the DAS-16, configured with a ± 5 V range, was used to collect data from the photodetector preamplifier. The TTL output from the filter disk timing tab was input as a digital signal to allow measurement of the filter disk period, gate the A/D converter, and synchronize data collection.

The required A/D sampling rate was approximately 10 kHz, based on the geometry of the CVF, a 10 Hz maximum speed of the filter disk, and a desire to obtain reflectance data on a 5 nm maximum spacing. A program was written in compiled BASIC to transfer the A/D data directly to an array while simultaneously allowing the counter operation needed to time the rotation of the filter disk. The program allowed data from up to 100 revolutions of the filter disk to be acquired, displayed for rapid visual verification, and stored on disk for later analysis.

The data acquisition program was tested to determine the maximum reliable sampling rate above which sample timing errors would become unacceptable. Two function generators were used to simulate the outputs of the spectrophotometer. The TTL output of one generator simulated the gating signal from the timing tab on the filter disk, and also triggered the second function generator which simulated the analog output of the photodetector preamplifier by means of a sine wave. Over the range from 2 kHz to 12.5 kHz the reliability of the data acquisition process was very good, with an error rate of less than 10 out of 5,000 scans (0.2%) in all cases, and no discernable trend of error rate versus sampling rate (table 1). A 15.2 kHz sampling rate was too fast for the system, causing an error rate of over 20%. Based on these tests, the data acquisition program was configured with a 10 kHz sampling rate, allowing a margin of safety before the point where the frequency of errors became unacceptable.

OPTICAL PERFORMANCE TESTS AND CALIBRATION

Once the prototype NIR spectrophotometer was operational, a sequence of performance tests and calibrations was completed. The steps in this procedure were: (1) optimize values for such basic operating parameters as filter disk speed and sample distance;

(2) document and analyze the general response of the instrument with these settings; (3) calibrate instrument output in terms of percent reflectance and wavelength; and (4) test the performance of the calibrated system in terms of such characteristics as bandwidth and stability. Although the details of these steps were specific to the instrument being developed, the general structure of this sequence could be applied to any reflectance instrument.

DETECTOR RESPONSE

The manufacturer's specifications for the PbS photodetector reported a typical time constant (the time required for the response to a step input to reach 63% of its final value) of 250 µs and a maximum time constant of 400 µs for an uncooled detector. At the design filter disk speed of 10 Hz, this time constant would correspond to 13 nm to 21 nm and would cause some filtering of the reflectance signal. To minimize the degree of filtering and maximize the signal, the detector output should reach its final value (or very nearly so) during the time that the theoretical pulse of light from the 2 mm entrance slit was incident on any one point on the CVF.

To test the detector response, a window was fabricated in the filter disk directly opposite the CVF segment (fig. 2). During normal operation, this window was completely shuttered, but for detector response testing a special shutter with two openings was installed. The first opening to pass by the light source during operation was a narrow slit 1 mm wide × 10 mm long. The second opening was a radial segment of a ring, approximately 10 mm × 10 mm. The first opening was designed to allow measurement of the pulse response of the detector by approximating the pulse width caused by the interaction of the entrance slit and a point of interest on the CVF, while the second, wider opening was designed to allow the settled response of the detector to be quantified. Detector output from a standard ceramic reflecting surface was recorded at filter disk periods from 100 ms to 300 ms. The 1 mm pulse response was normalized by the settled response from the 10 mm opening (fig. 4). As a compromise between the increasing signal level with longer disk period and the desire to collect data as quickly as possible for field operation, a filter disk period of 200 ms (speed of 5 Hz) was selected for subsequent tests.

Table 1. Number of bad data scans out of 5000 total scans at various A/D sampling rates

Sampling Rate (kHz)	Number of Bad Scan
2.0	8
5.0	6
5.5	8
6.7	10
8.0	3
10.0	5
12.5	7
15.2	> 1000
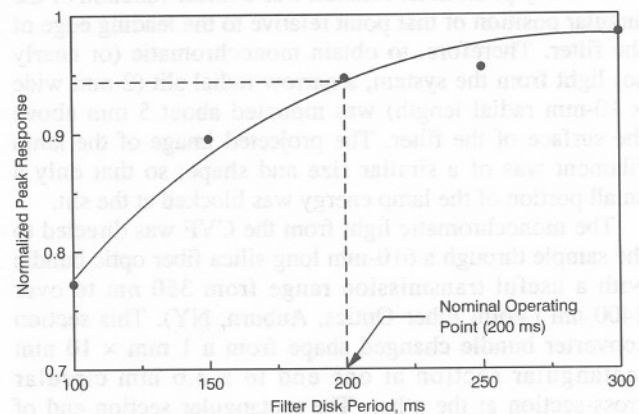
Figure 4–Relationship between photodetector response and filter disk period.

SAMPLE DISTANCE EFFECTS

To determine the optimum operating distance from the sample surface, the location of the sensing head was varied from 6.4 mm to 25.4 mm above a ceramic standard and the output signal recorded (fig. 5). Although operation at the minimum distance would provide the strongest signal possible, it would have two negative effects. In a field unit some allowance would be needed to compensate for variations in instrument-to-sample distance. Decreasing this distance would also decrease the area of the sample being sensed. For a nonuniform material such as soil, sensing of a relatively larger area would be desirable to average out any signal differences caused by sample heterogeneity. As a compromise between signal strength and these two effects, a nominal operating distance of 15 mm was selected.

SYSTEM OUTPUT CHARACTERISTICS

The general output characteristics of the system were documented at a filter disk speed of 5 Hz. A ceramic disk was used as the reflectance object due to its nearly constant reflectance over the wavelength range of interest. The digitized signal obtained for a typical ceramic disk reflectance scan (fig. 6) exhibited several noteworthy features. The rapid signal rise near A/D sample point 500 occurred as the leading edge of the CVF passed the entrance slit. The roll-off of the response with increasing A/D point number (and increasing wavelength) was due to the transmission characteristics of the fiber optic bundle and possibly the illumination characteristics of the lamp. Several nonlinearities were present in the signal, most notably a notch near point 700 likely due to the presence of some unidentified absorber in the optical system.

Another characteristic of the response curve was the non-zero baseline found in the non-illuminated portions of the scan (outside the range from about point 500 to point 875). This non-zero, dynamic baseline was caused by the ac coupling of the detector output in the preamplifier (fig. 3). The ac coupling eliminated possible long-term drift problems and allowed optimal use of the available A/D range. However, this ac coupling required application of a software correction to adjust the digitized reflectance data to a zero baseline.

The output signal of the instrument with no illumination provided an indication of the amount of excitation-
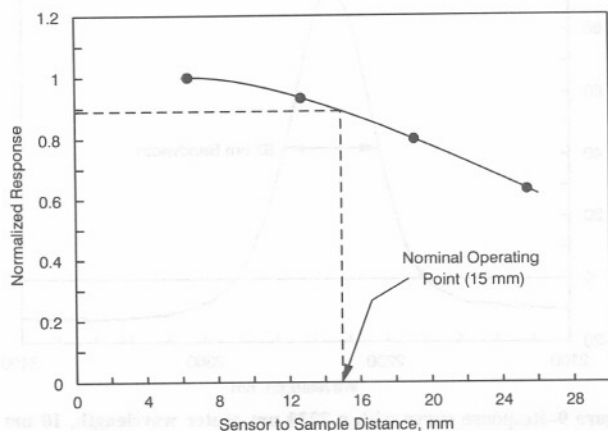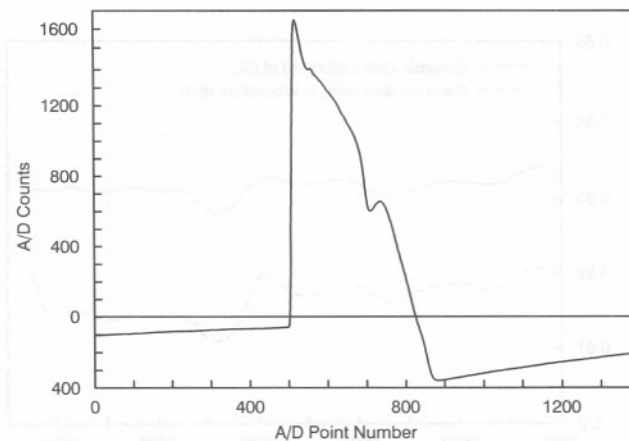
Figure 6–Digitized signal for a typical ceramic disk reflectance scan.

independent noise present in the data. The noise was quite small in magnitude, approximately 2 A/D counts or 0.1% of the full-scale reflectance signal, and consisted of a high-frequency random noise superimposed on a 60 Hz sine-wave. With no radiation incident on the detector, a positive offset of approximately 5 A/D counts was observed.

CERAMIC DISK REFERENCE CALIBRATION

To compensate for changes in illumination, detector response, and other optical system variations, each sensor reading was referenced to the reading from a ceramic disk, a substance widely accepted for standardization of NIR instruments. The ceramic reference also enabled conversion of the instrument response to a percent reflectance (or decimal reflectance) basis.

Two nominally identical ceramic disks were used in the calibration procedure. One 50-mm diameter disk was used as the working reflectance standard for the prototype spectrophotometer, while the other disk was sent to the USDA-ARS Instrumentation and Sensing Laboratory, where its reflectance characteristics were obtained by comparison with a standard sample of slightly compressed sulfur (fig. 7). A series of 10 paired readings of both ceramic disks was then completed with the prototype spectrophotometer and used to compute the decimal reflectance characteristics of the ceramic disk used for sensor calibration (fig. 7).

WAVELENGTH CALIBRATION

During early laboratory tests, a significant amount of sub-periodic filter disk speed variability was observed. Relocation of the filter disk timing tab (fig. 2) reduced this variability by providing timing references as close as possible to the beginning and to the end of the analog reflectance signal. The relocated timing tab provided the reference near the end of the reflectance signal, while the reference at the beginning of the signal was obtained from the half-peak point on the initial step response of the CVF (fig. 6). Each individual A/D point was then located at some fraction of the elapsed time between the initial reference and the final reference. This period, during which filter disk speed variations would reduce the accuracy of the wavelength calibration, was minimized at

Figure 5–Relationship between signal level and sample distance.
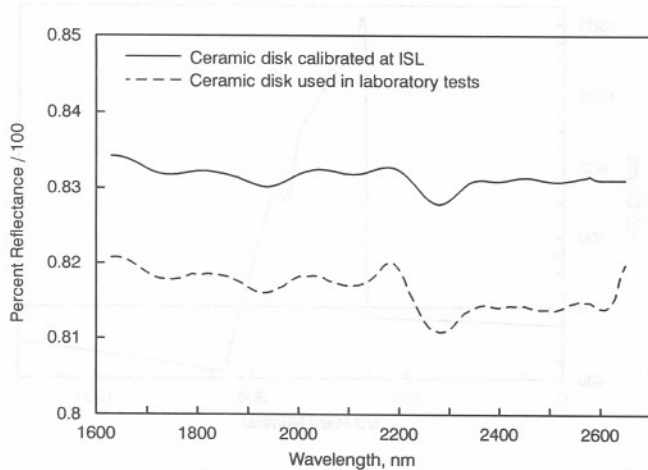
Figure 7–Reflectance characteristics of the ceramic reference disk scanned at the USDA-ARS Instrumentation and Sensing Laboratory (ISL) and the working ceramic reference disk used to calibrate the prototype spectrophotometer.

approximately 40% of the total filter disk period. The maximum uncertainty in wavelength estimation was approximately 2.5 nm.

Wavelength calibration was accomplished with a sheet of white polystyrene, a material with well-defined absorption bands in the NIR region (Williams, 1987). The major polystyrene absorption bands centered at 1682 nm, 2165 nm, and 2470 nm, identifiable in prototype sensor scans of the polystyrene sheet (fig. 8), were used in the calibration step. Each polystyrene dataset was ratioed with a paired ceramic reading to obtain reflectance data which was then processed to find the location of the absorbance peaks (or reflectance troughs). A linear regression was used to relate the location, in terms of fraction of the timing period, of the three polystyrene reflectance minima to their known wavelengths. An excellent correlation was found, with an r^2 of 0.99999 and a standard error of the wavelength estimate of 1.18 nm. Application of the wavelength calibration equation showed that the sensor had a usable data range from under 1650 nm to over 2650 nm, well in excess of the design requirement.
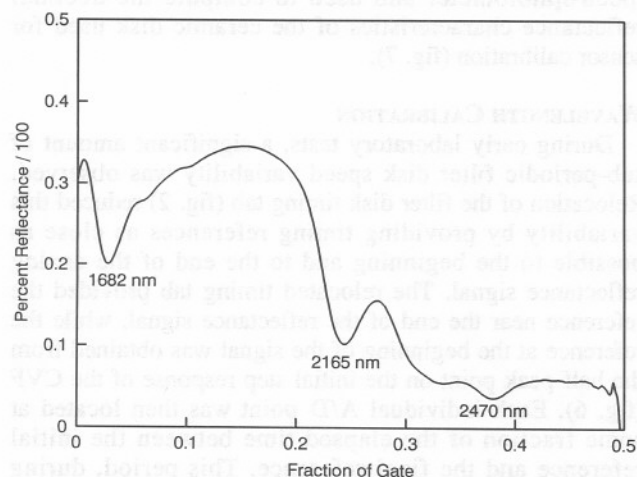
Figure 8–Typical polystyrene reflectance curve obtained with the prototype spectrophotometer.

BANDWIDTH DETERMINATION

The bandwidth of the CVF was investigated by inserting a fixed filter with a 2230 nm center wavelength and nominal 10 nm bandwidth in the optical path between the light source and the CVF. The halfpeak bandwidth of the reflectance curve of a ceramic standard was obtained at several filter disk periods with the fixed filter in place.

The apparent bandwidth of the CVF with the standard 200 ms period was 52 nm (fig. 9), within the system design requirements. The bandwidth with a 300 ms period was 50 nm, while with a 100 ms period it was 61 nm. The standard 2 mm entrance slit was not a limiting factor, as the CVF bandwidth remained at 52 nm when the slit width was decreased to 1 mm. The apparent bandwidth determined by this test was somewhat higher than the true bandwidth of the CVF, since the light illuminating the CVF was not monochromatic, but rather exhibited the 10 nm bandwidth of the fixed filter. A computer simulation using triangular filter functions predicted that the apparent bandwidth would be approximately 10% greater than the actual bandwidth. As this level of accuracy was sufficient, deconvolution to obtain the true CVF bandwidth was not attempted.

OPTICAL RESPONSE STABILITY

Variation in the optical response of the sensor was monitored by means of 10 repeated readings of the same ceramic disk over a 2-h period. Little variation was seen when comparing the baseline corrected mean sensor readings. To magnify any differences present, each reading was normalized by dividing the response pointwise by the ceramic response measured at the beginning of the 2-h period. Two types of variation (fig. 10) were seen in the normalized response curves as compared to the unity response which would have been obtained with a perfectly stable system. An approximately constant offset was observed in the 1650 to 2100 nm portion of the curve, indicating a drift in the lamp output or other optical characteristics of the system.

More variation was seen in the portion of the curve past 2100 nm, most notably a peak or trough located near 2200 nm, a location corresponding to the notch in the
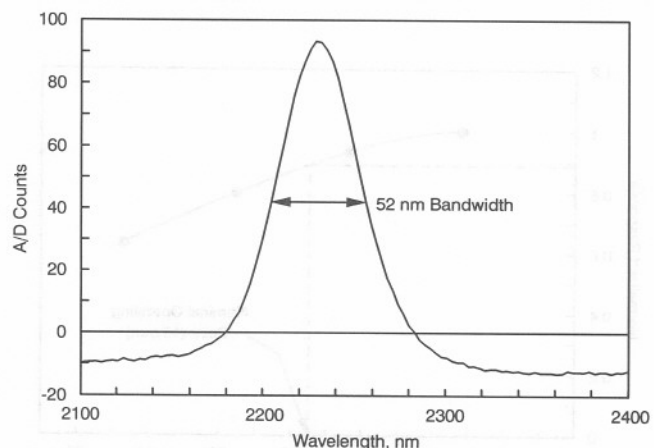
Figure 9–Response curve with a 2230 nm center wavelength, 10 nm bandwidth filter placed in the optical path, showing the 52 nm apparent half-amplitude bandwidth of the system.
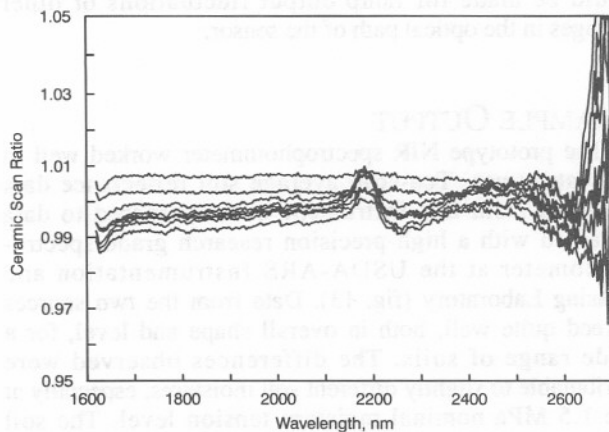
Figure 10–Ten readings of the same ceramic disk during a 2 h stability test, normalized by ratioing each successive curve to the first (time zero) reflectance curve.

system response curve (fig. 6). These variations between scans were due to sub-periodic variations in the filter disk speed, which caused the calibration between wavelength and A/D sample point to shift. The influence of a given wavelength shift on sensor output was magnified in portions of the response curves with steeper slopes and with rapidly changing slopes such as the notch area noted above.

To verify this relationship, a ceramic scan was referenced to itself, with wavelength shifts of up to 5 nm in each direction. The results of this simulation (fig. 11) were very similar in shape to the deviations observed between successive ceramic readings (fig. 10), providing additional evidence that the majority of the non-offset difference between ceramic readings was attributable to sub-periodic variations in filter disk speed.

DATA PROCESSING ALGORITHMS

A sequence of operations was necessary to convert the raw digitized data obtained from the spectrophotometer and stored by the data collection program to the percent
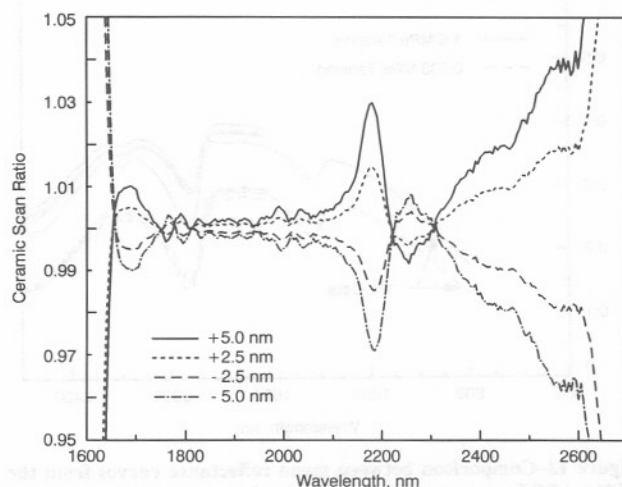
Figure 11–The effect of wavelength offset on the ratio of a ceramic reflectance curve to itself.

reflectance data needed to calibrate the instrument and to estimate soil properties.

BASELINE CORRECTION

A dynamic baseline correction algorithm was developed to convert the ac coupled raw reflectance signal (fig. 6) to a dc signal with a baseline level of zero A/D counts. Referring to the schematic of the detector and preamplifier (fig. 3), the parameter which varied directly with the radiation incident on the detector was the current through the photodetector, i_{in}. The parameter digitized by the data collection system was the voltage output of the preamplifier, V_{out}. Analysis of the preamplifier circuit showed that the general relationship between these two parameters was given by:

$$i_{in} = k_1 + k_2 V_{out} + k_3 \int V_{out} dt \quad (1)$$

The output voltage, V_{out}, was converted to raw A/D counts, D_{raw}, by application of a gain and offset in the digitization process:

$$D_{raw} = a_0 + a_1 V_{out} \quad (2)$$

$$V_{out} = a_3 + a_4 D_{raw} \quad (3)$$

D_{raw} was the parameter stored as data by the computer. However, the desired reading was the corrected A/D counts, D_{corr}, which represented the digitization of the input current. A sequence of steps was required to calculate D_{corr} from D_{raw}. Equation 1 was digitized and rewritten with D_{raw} replacing V_{out} and D_{corr} replacing i_{in}:

$$D_{corr} = c_1 + c_2 D_{raw} + c_3 \sum_1^n D_{raw} + c_4 \quad (4)$$

Equation 4 was simplified by setting c_2 to one, since the units of D_{raw} were the same as the units of D_{corr}. Also, c_4 was removed from under the summation:

$$D_{corr} = D_{raw} + c_1 + c_4 n + c_3 \sum_1^n D_{raw} \quad (5)$$

Calculation of D_{corr} from D_{raw} then required values for c_1, c_3, and c_4 to be determined. These values varied with each particular data curve, due to the differences in reflected energy between samples. To determine c_1, c_3, and c_4 it was necessary to make use of the fact that D_{corr} should, on the average, be zero in the baseline portions of the curve (from points 1 to 500 and 875 to 1400 in fig. 6). In these two portions of the data curve, equation 5 could be rewritten as:

$$D_{raw} = -c_1 - c_4 n - c_3 \sum_1^n D_{raw} \qquad (6)$$

Equation 6 was fit to the data in the baseline areas of the curve using a least-squares multiple linear regression, where the independent variables at each data point were the index number of the data point and the summation of the raw A/D data up to that point. The dependent variable was the raw A/D data value. The regression was applied to a 167-point section of the baseline on either side of the data portion of the curve, corresponding to 16.67 ms at the 10 kHz sampling rate, to account for the mean of any 60 Hz noise present in the data. An excellent fit to the raw baseline data was obtained, with typical r^2 values exceeding 0.999. Once c_1, c_3, and c_4 were determined, equation 5 was then applied pointwise to the raw A/D data to generate the baseline corrected data curve (fig. 12).

WAVELENGTH CALIBRATION

The polystyrene wavelength calibration equation was applied to the data to convert A/D point number to the corresponding wavelength.

DATA POINT INTERPOLATION

Due to wavelength calibration differences and variations in filter disk period, a given A/D point did not correspond to the same wavelength for all reflectance readings. Therefore, the baseline corrected sensor response data were interpolated to a standard wavelength spacing for pointwise differencing of soil and ceramic readings and additional analysis. Points were generated every 5 nm from 1600 nm to 2700 nm using piecewise cubic spline interpolation algorithms (Spath, 1974).

REFLECTANCE CALCULATION

The interpolated, baseline corrected raw data obtained from the sensor were converted to decimal reflectance (percent reflectance ÷ 100) by comparison against data obtained from the ceramic disk with known reflectance characteristics (fig. 7). Repeated readings of the ceramic disk were done on a frequent basis, so that compensation
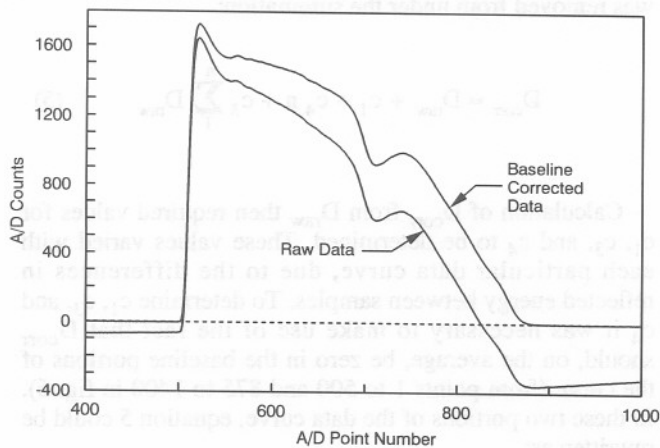
could be made for lamp output fluctuations or other changes in the optical path of the sensor.

EXAMPLE OUTPUT

The prototype NIR spectrophotometer worked well in laboratory use. Ten-scan average soil reflectance data obtained from this instrument were compared to data obtained with a high-precision research grade spectrophotometer at the USDA-ARS Instrumentation and Sensing Laboratory (fig. 13). Data from the two sources agreed quite well, both in overall shape and level, for a wide range of soils. The differences observed were attributable to slightly different soil moistures, especially at the 1.5 MPa nominal moisture tension level. The soil organic matter estimates obtained by application of multivariate calibration techniques to these data were insensitive to the reflectance differences induced by changes in soil moisture content (Sudduth, 1989).

SUMMARY AND CONCLUSIONS

A portable, near-infrared spectrophotometer intended for in-field use was designed, fabricated, and performance tested in the laboratory. The intended use of this device was rapid estimation of soil organic matter as a control input for variable rate herbicide application, using previously developed methods (Sudduth and Hummel, 1991).

Significant features included a circular variable filter monochromator for ruggedness and simplicity of operation, fiber optic coupling for sensing of remote samples, and a software algorithm which corrected the ac-coupled instrument readings to a zero baseline. Performance tests documented a sensing range of 1650 to 2650 nm, an optical bandwidth of under 55 nm, and an optimal data acquisition rate of 5 Hz. Soil reflectance curves obtained with this instrument in the laboratory agreed well with data obtained using a research grade spectrophotometer.

Figure 12–Typical raw ceramic reflectance curve and the same curve after application of the baseline correction algorithm.
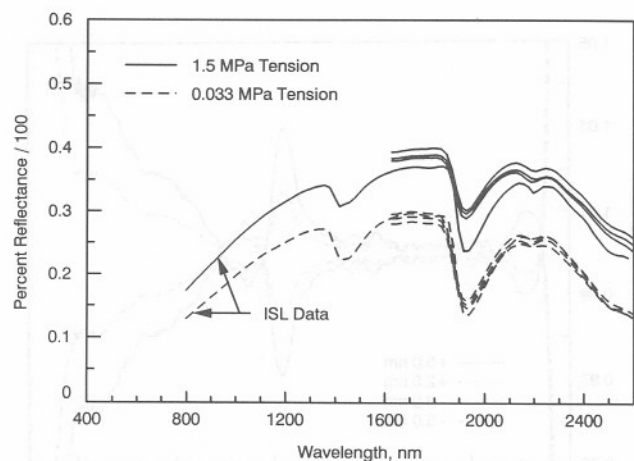
Figure 13–Comparison between mean reflectance curves from the USDA-ARS Instrumentation and Sensing Laboratory (ISL) and three replicate prototype spectrophotometer curves for Ade Loamy Sand at two moisture tension levels.

REFERENCES

Dalal, R. C. and R. J. Henry. 1986. Simultaneous determination of moisture, organic carbon, and total nitrogen by near infrared reflectance spectrophotometry. *Soil Sci. Soc. Am. J.* 50:120-123.

Gaultney, L. D., J. L. Shonk, D. G. Schultze and G. E. Van Scoyoc. 1989. A soil organic matter sensor for prescription chemical application. In *Agricultural Engineering – Proceedings of the 11th International Congress*, Dublin, 4-8 September 1989, eds. V. A. Dodd and P. M. Grace, 3065-3072. Rotterdam: Balkema.

Gunsaulis, F. R., M. F. Kocher and C. L. Griffis. 1991. Surface structure effects on close-range reflectance as a function of soil organic matter content. *Transactions of the ASAE* 34(2):641-649.

Henderson, T. L., A. Szilagyi, M. F. Baumgardner, C. T. Chen and D. A. Landgrebe. 1989. Spectral band selection for classification of soil organic matter content. *Soil Sci. Soc. Am. J.* 53:1778-1784.

Hovis, W. A., Jr., W. A. Kley and M. G. Strange. 1967. Filter wedge spectrometer for field use. *Appl. Optics* 6(6):1057-1058.

Jauch, K. M. 1979. A portable rapid spectrophotometer for colour studies. *J. Physics E: Sci. Instrumentation* 12:1171-1175.

Krishnan, P., J. D. Alexander, B. J. Butler and J. W. Hummel. 1980. Reflectance technique for predicting soil organic matter. *Soil Sci. Soc. Am. J.* 44:1282-1285.

McClure, W. F. 1987. Near-infrared instrumentation. In *Near-infrared technology in the agricultural and food industries*, eds. P. C. Williams and K. H. Norris, 89-106. St. Paul, MN: American Association of Cereal Chemists.

Schreier, H. 1977. Quantitative predictions of chemical soil conditions from multispectral airborne, ground, and laboratory measurements. In *Proc. 4th Canadian Symposium on Remote Sensing,* 106-112. Ottawa: Canadian Aeronautical and Space Institute.

Spath, H. 1974. *Spline Algorithms for Curves and Surfaces*. Winnipeg: Utilitias Mathematica Publishing.

Sudduth, K. A. 1989. Near infrared reflectance soil organic matter sensor. PhD. diss., University of Illinois, Urbana-Champaign. Public. No. 90-15736. Ann Arbor MI: University Microfilms, Inc. (Diss. Abstr. Int. B 51(1):308).

Sudduth, K. A. and J. W. Hummel. 1991. Evaluation of reflectance methods for soil organic matter sensing. *Transactions of the ASAE* 34(4):1900-1909.

Williams, P. C. 1987. Commercial near-infrared reflectance analyzers. In *Near-infrared technology in the agricultural and food industries,* eds. P. C. Williams and K. H. Norris, 107-142. St. Paul, MN: American Association of Cereal Chemists.

Worner, C. R. 1989. Design and construction of a portable spectrophotometer for real time analysis of soil reflectance properties. Unpublished M.S. thesis, Library, University of Illinois, Urbana-Champaign.